

Effective Removal of the Direct Black-38 Dye from Wastewater Using a New Silica-Modified Resin: Equilibrium and Thermodynamics Modeling Studies

Ranjhan Junejo,* Shahabuddin Memon, and Savas Kaya

Cite This: <https://dx.doi.org/10.1021/acs.jced.0c00292>

Read Online

ACCESS |



Metrics & More

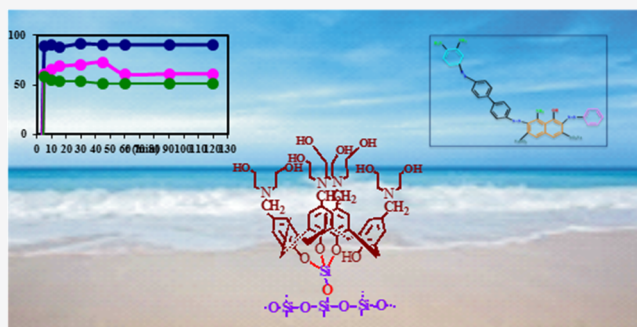


Article Recommendations



Supporting Information

ABSTRACT: In this study, the synthesis of *p*-diethanolaminomethylcalix[4]arene and its immobilization on a silica surface have been performed for the removal of the direct black (DB-38) dye from wastewater samples. The newly synthesized *p*-diethanolaminomethylcalix[4]arene-immobilized silica (DIS) resin has been analyzed and characterized by FTIR spectroscopy and SEM techniques. To check the efficiency of the DIS resin, batch and column adsorption procedures have been applied under the optimized parameters, i.e., resin dosage, pH, and temperature. To validate the experimental data, Langmuir, Freundlich, and D-R models have been applied. The results show that adsorption follows the Freundlich model well with a good correlation coefficient ($R^2 = 0.999$). Moreover, the energy E (kJ/mol) was calculated with the help of the D-R model, which suggested that the adsorption has an ion exchange nature. The DIS resin was also applied to real industrial samples of DB-38 dye wastewater. The results show that the DIS resin removes 99% of the dye successfully. Thermodynamics studies were conducted to know the feasibility and the mechanism of the adsorption reaction. The thermodynamic parameters show that the adsorption is spontaneous and exothermic. The theoretical calculation was performed at the B3LYP/DZP calculation level of the ADF program, and the power of the interaction between adsorbent and dye molecules can be determined in the light of chemical reactivity analysis.



1. INTRODUCTION

Water pollution caused by the discharge of industrial effluents has caused a number of diseases in human beings and aquatic life.¹ These industrial effluents generally contain water pollutants, which may be organic dyes, metal ions, antibiotics, chemicals, and many more.² Among different pollutants, water contaminated by synthetic dyes has severe poisonous effects on human health.³ Dyes are basically organic synthetic compounds, also called as organic colorants. They can be synthesized by the reaction with aromatic compounds, mostly phenol or aromatic amines and diazonium salt having the functional group $R-N_2^+X^-$.⁴ The azo dyes have many important applications in textile, synthetic fiber, dyeing, and paint industries. The plastic, paper, and glass industries as well as many others use dyes to enhance and increase the beauty of their products.⁵ Due to the increased consumption of azo dyes, more than 10,000 different dyes have been synthesized in the world that produced about 70,000 metric tons of dyes per year.⁶ However, it is estimated that 10–15% of total dyes have been discharged into fresh water by different industries during the dyeing process, which contains various types of unreacted dyes.⁴

Dye molecules have complex structures that could be reduced into aromatic amines by the cleavage of the azo group

due to weather conditions.⁷ The synthetic basis and their conversion into aromatic amines help them resist degradation because the benzidine group is formed. Therefore, these aromatic amines are carcinogenic in nature. Consequently, above 500 azo dyes having a carcinogenic amine origin are recognized as toxic pollutants and must be removed.⁵

Thus, keeping in view the toxicity of dyes, different techniques have been developed; however, adsorption remains to be the more effective method as compared to others.⁸ Adsorption is a very simple and cheaper method that is based upon a very basic principle where a particular species, which may either be a negative or positive ion or a neutral molecule, binds to a solid surface, which also has particular functionalities and binding sites.^{9,10} Therefore, different adsorbents such as silica-based polymers, activated carbon, peat, chitin, and many other commercially available adsorbent were used previously by many researchers throughout the world.^{11–13} Mostly, the

Received: March 30, 2020

Accepted: September 1, 2020



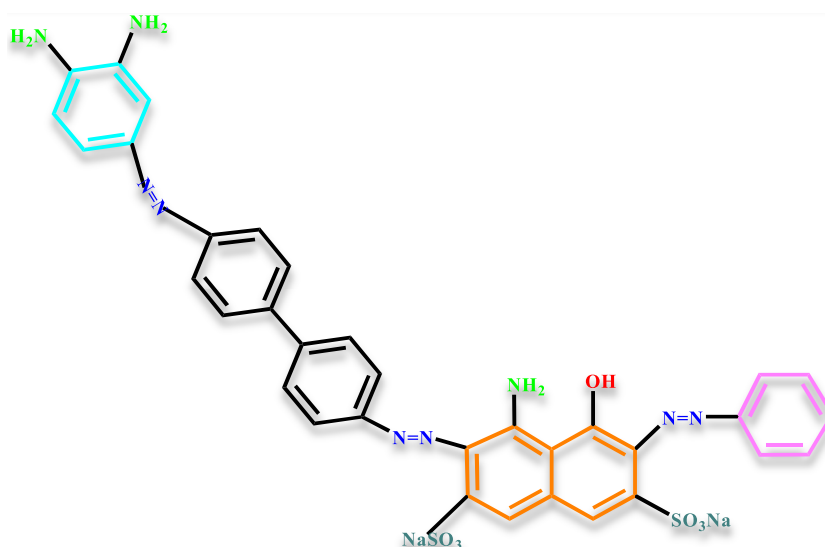


Figure 1. Chemical structure of the direct black (DB-38) azo dye.

adsorbents used have less selectivity and sensitivity and/or are not regenerable. In the adsorption process, the adsorbent should be selective and sensitive and have the ability to be regenerated again and again.^{12,14–19}

In this regard, calixarenes are used as a typical class of host molecules. Basically, calixarenes are a class of cyclic oligomers that can be formed by a base-catalyzed reaction between phenol and formaldehyde. Calixarenes have an upper and lower narrow rim, which can be functionalized with different organic functional groups. The selectivity for recognition of host species depends upon the functional groups present in the host. Due to easy functionalization, calixarenes have a number of applications in different fields of science and technology such as catalysis, adsorbents, sensors, and so on.^{20,21} Furthermore, chemical modification of polymeric materials such as silica with calixarenes provides a better adsorbent that is selective, sensitive, thermally stable, and regenerable.^{22,23} The silica surface can be modified with piperidine-based calix[4]arene for the removal of the reactive blue 19 dye from wastewater.²³ This study also focuses on the synthesis of *p*-diethanolaminomethylcalix[4]arene and its chemical attachment onto a silica surface to prepare a new resin for the removal of the toxic azo dye direct black (DB-38) from wastewater (Figure 1).

2. EXPERIMENTAL WORK

2.1. Materials and Methods. **2.1.1. Chemicals.** A list of the chemicals used in the experimental work is provided in Table 1.

The DB-38 dye was obtained from Merck and prepared according to its required concentration in deionized water. The dye-contaminated water samples were collected from local textile and dyeing industries of the Jamshoro Sindh-Pakistan district. The pH of the DB-38 solution was adjusted using 0.1 N HCl or NaOH. All other chemicals used during the experimental work were of analytical grade and GR grade. Silica gel (230–400 mesh) was purchased from sigma Aldrich.

2.1.2. Apparatus. All synthesized compounds were analyzed by CHNS elemental analysis, melting point determination, FTIR spectroscopy, and SEM techniques. A CHNS elemental analyzer (model Flash EA 1112, 20,090-Rodano, Milan, Italy)

Table 1. List of Chemicals Used in Experimental Work

name of chemical/reagent	supplier	% purity
toluene	Merck: CAS no.: 0000108883	99.8%
dichloromethane	Supelco: CAS no.: 0000075092	99.8%
chloroform	SAFC CAS no.: 0000067663	99.8%
4- <i>tert</i> -butylphenol	Sigma: CAS no.: 0000098544	99%
formaldehyde (37%) solution	SAFC: CAS no.: 0000050000	5–10% stabilizers
sodium hydroxide	Sigma: CAS no.: 0001310732	99%

was used for the elemental analysis, while the melting points were determined using a Gallenkamp apparatus model (MFB. 595. 010 M, England). A Thermo Nicolet 5700 FT-IR spectrometer (WI. 53,711, USA) was used to record the IR spectra. An SEM technique (JSM-6380) was applied onto the DIS resin to characterize its surface morphology. A Quanta Chrome ASiQwin surface area analyzer was used to examine the surface area, pore size, and pore volume.

2.2. Synthesis. **2.2.1. Synthesis of *p*-Diethanolaminomethylcalix[4]arene.** The synthesis of compounds 1 and 2 was performed via reported procedures,^{24–26} while compound 3 was synthesized by the following method, which is given in Figure 2.

In a 100 mL round-bottom flask, 2.0 g of compound 2 was solubilized in 50 mL of tetrahydrofuran (THF) solution and stirred at room temperature till the reaction mixture becomes clear. After that, the reaction flask was placed into an ice bath and the reaction mixture was cooled with its temperature maintained below 273 K by addition of crushed ice into the reaction bowl. After maintaining the temperature, 5 mL of acetic acid and 1 mL of HCHO were added, the mixture was stirred for 15 min, then 3 mL of diethanolamine was added, and the stirring was continued. The completion of reaction was monitored by using basic analytical techniques such as TLC and FTIR spectroscopy. After confirmation of completion, the reaction flask was removed, 15 mL of water was added, the solution was shaken till the solid precipitate was completely solubilized and extracted with diethyl ether three times, then

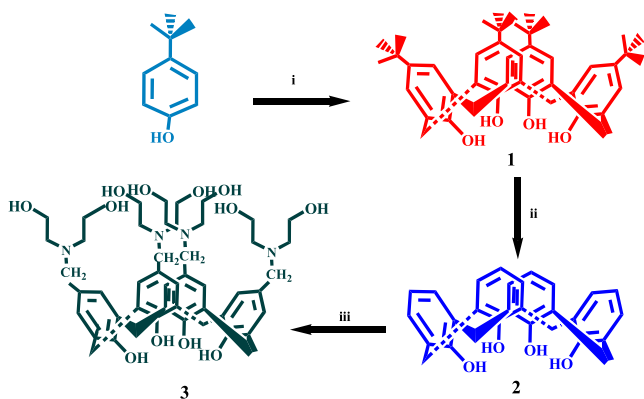


Figure 2. Synthesis scheme of *p*-diethanolaminomethylcalix[4]arene (3). Reagents: (i) NaOH/HCHO, (ii) AlCl₃/phenol, and (iii) diethanolamine/HCHO/acetic acid.

20 mL of 10% K₂CO₃ solution was added, and the product was filtered. After drying and recrystallization, white crystals were obtained and weighed and the % yield was calculated.

2.2.2. Synthesis of DIS Resin. The DIS resin was prepared by the modification of the silica surface by attachment of compound 3, as shown in Figure 3. Therefore, 5 g of silica was

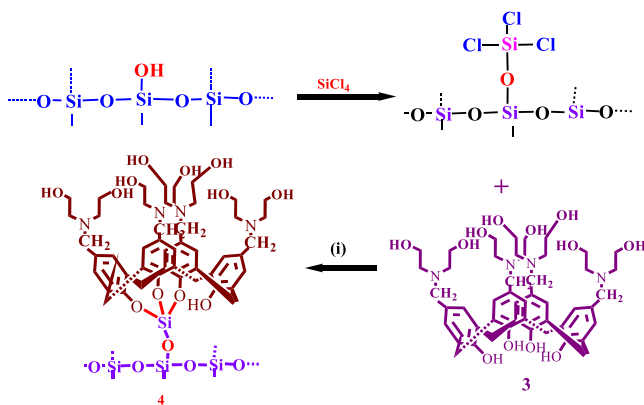


Figure 3. Synthesis route of the DIS resin.

weighed, treated with 0.1 M HCl, then washed with deionized water, and dried at 393 K for 3 h. After cooling the silica, 50 mL of 0.01 M SiCl₄ solution and 10 mL of triethylamine were added, resulting in a cloudy solution mixture, which was placed at room temperature for 6 h. After removing the solvent by vacuum, 1.5 g of compound 3 solubilized in chloroform was poured into it followed by addition of 8 mL of triethylamine, and the mixture was refluxed at 523 K. The reaction was monitored by FTIR spectroscopy. After 36 h, grayish resin 4 was filtered, washed with 150 mL each of chloroform, methanol, and finally water, and dried.

2.3. Adsorption. **2.3.1. Batch Adsorption.** The batch adsorption study was performed to analyze the DB-38 dye adsorption potential of the DIS resin. During adsorption experiments, the resin amount, pH of DB-38 dye solution, and contact time were optimized and the role of electrolyte and the temperature effect were determined. A dye solution (10 mL, 2×10^{-5} mol/L) with 60 mg of DIS resin was placed onto a mechanical shaker at a speed of 130 rpm for 1 h. After 1 h, the DIS resin was filtered and the concentration of remaining DB-38 was analyzed using a UV-vis spectrophotometer. The % adsorption of DB-38 was determined using eq 1.

$$\% \text{adsorption} = \frac{C_i - C_f}{C_i} \times 100 \quad (1)$$

In this equation, C_i and C_f stand for the initial and final concentrations of the DB-38 dye. The amount of dye (q_e in mol/g) adsorbed onto the DIS resin can be calculated using eq 2.

$$q_e = \frac{(C_i - C_e)V}{m} \quad (2)$$

In eq 2, C_i and C_e are the initial and final concentrations (mol/L) while V is the volume (mL) of the DB-38 solution and m is the weight (in g) of the DIS resin.

3. RESULTS AND DISCUSSION

3.1. FTIR Spectroscopy. FT-IR spectroscopy is the most important technique to identify the functional group present in a compound. The chemical modification of the silica surface was confirmed by FT-IR spectroscopy to analyze the functional groups.^{27,28} Therefore, the synthesized compounds were analyzed by FTIR spectroscopy, as shown in Figure 4. The spectrum in Figure 4a is for *p*-diethanolaminomethylcalix[4]arene, which comprises some characteristic bands at 3351, 2914, 1680, 1288, and 1027 cm⁻¹ for OH, C-H, C=C, C-N, and C-O stretching, respectively while the peak at 1388 cm⁻¹ is attributed to C-OH bending. The spectrum in Figure 4b is for pure silica powder, which has characteristic peaks at 3479 and 1614 cm⁻¹ attributed to OH and Si-O stretching while that at 1076 cm⁻¹ is attributed to Si-OH bending peak. The spectrum in Figure 4c is for the DIS resin, which has some new bands at 3404, 2921, and 1457 cm⁻¹, which are peaks attributed to OH, C-H, and C=C vibrations and the peak at 1084 to OH bending. These additional new peaks found for silica confirm the immobilization of compound 3 onto the silica surface.

3.2. SEM Characterization of the DIS Resin. Scanning electron microscopy is the most versatile technique to analyze the surface of materials.²⁹ Therefore, the DIS resin was characterized by an SEM technique as shown in Figure 5. Figure 5a is the image of pure silica, which is smooth and crystalline and has a specific geometry. Meanwhile, Figure 5b is the SEM image of the DIS resin (4), which is obtained after the attachment of compound 3 onto the silica surface. The roughness observed in the image of Figure 5b is due to the attachment of compound 3 onto the silica surface. Such a type of material was also prepared in previous studies for the adsorption of RB-5, RR-45, and DB-38 dyes.^{27,28} Moreover, the DIS resin particles look smaller in size as compared to those of silica in Figure 5a and a smaller particle size will lead to a larger surface area and make the material be able to remove more analytes.

3.3. Pore Size Distribution (PSD). The PSD of the DIS resin from their nitrogen adsorption isotherms was determined by applying the ASiQwin and non-local density functional theory (NLDFT) model in SAIEUS. The nitrogen adsorption-desorption isotherms at 77 K are given in Figure 6, which shows a type-IV isotherm in the range of 0.6–0.9 P/P_0 , and the specific surface area calculated by the BET technique was 27.8630 m²/g. The calculated PSDs clearly show that the porous structure of the DIS resin in 2D-NLDFT mode has a less than 3 nm pore size.

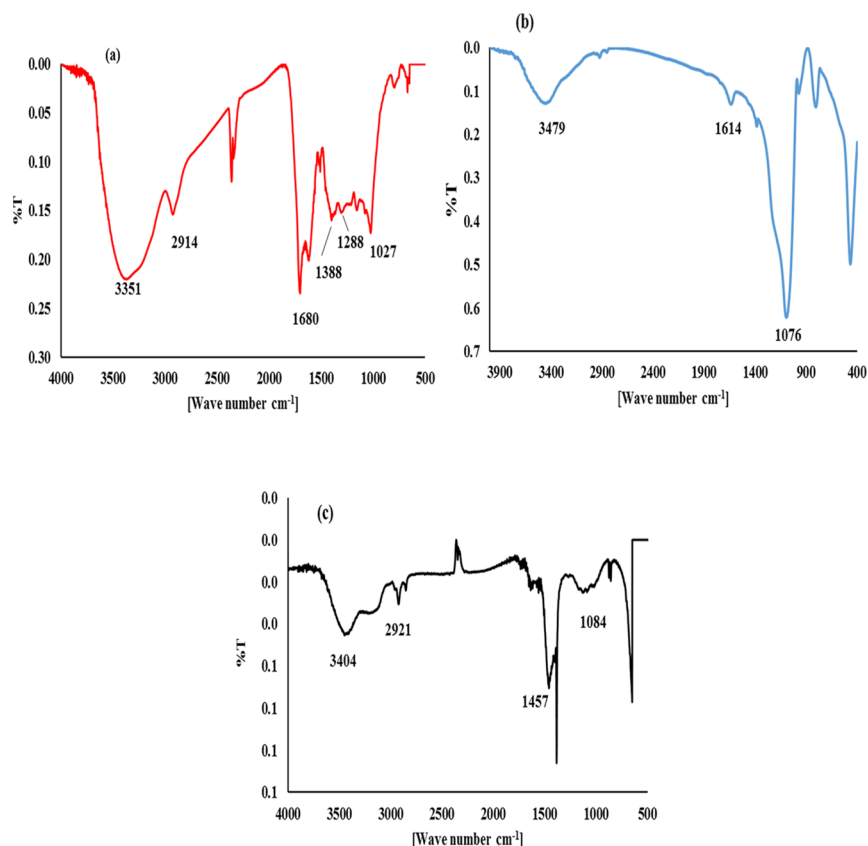


Figure 4. FTIR spectrum of (a) *p*-diethanolaminomethylcalix[4]arene, (b) pure silica, and (c) the DIS resin.

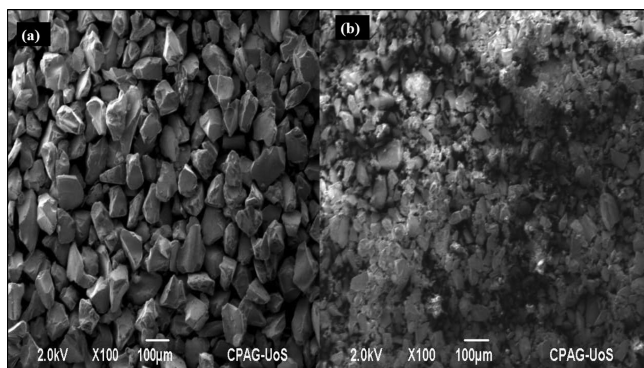


Figure 5. SEM images of (a) silica and (b) the DIS resin (after modification of the silica surface).

4. ADSORPTION PARAMETERS

4.1. Effect of Adsorbent Dosage. To optimize the DIS resin dosage, different experiments were performed ranging from 10–100 mg/L DIS resin dosages given in Table S1 and Figure 7. During the adsorption, it was observed that increasing the amount of DIS resin, the % adsorption increases due to the increasing amount of binding sites of the DIS resin for the DB-38 dye molecule. It is clear in Figure 7 that 99.1% of the DB-38 dye was removed using only 60 mg of DIS resin; increasing further the dosage was found to have no significant effect on the % removal of the DB-38 dye. In the literature, a similar phenomenon has been observed for the adsorption of RB-19,^{23,30} MB,³¹ Evans blue, and Chicago sky blue B6.³²

4.2. Optimization of pH. The % removal of the DB-38 dye from water depends on the pH value, which plays a

significant role in the entire adsorption process because it affects the adsorbate and adsorbent binding sites. In this regard, the effect of pH from acidic to basic has been investigated, which is given in Table S2 and Figure 8. In Figure 8, it is noticed that the % removal decreases with increasing pH and maximum % removal was achieved at pH 3. Below pH 3, there is no significant difference in % removal, and above pH 3, % removal decreases. Thus, at acidic pH, the sulfur and amine groups of the DB-38 dye molecule are protonated and can attract electron-donating groups present in the DIS resin. Similarly, OH groups in the DIS resin become active and attract the negative part of the DB-38 dye and the overall net charges tightly bind the dye molecule to the DIS resin. Previously, different studies were performed using other dyes such as Evans blue and Chicago sky blue B6, which were removed successfully using carboxylic calix[4]arene magnetic (CCM) nanoparticles at pH 2.5.³² Another study was performed using 25,26,27,28-tetrakis-(*N,N*-diethyl-1,2-aminoethylamidomethoxy)-calix[4]arene-based Amberlite XAD-4 resin for the effective removal of MO and MR dyes from water at pH 3.³³ The novel derivative pyrazine-2-carboxylate-substituted calix[4,8]arene was used for the removal of reactive black (RB-5), trapeolin 000 (TP), Evans blue (EB), and Chicago sky blue at pH 3.³⁴

4.3. Effect of Temperature and Time. The temperature has a great role in the removal of the DB-38 dye as a function of contact time between the DIS resin and dye molecules. Therefore, adsorption of the DB-38 dye has been examined at various temperatures (293–308 K), as given in Table S3 and Figure 9, and it has been noticed that % removal decreases with the increase in temperature from 293–303 K, which

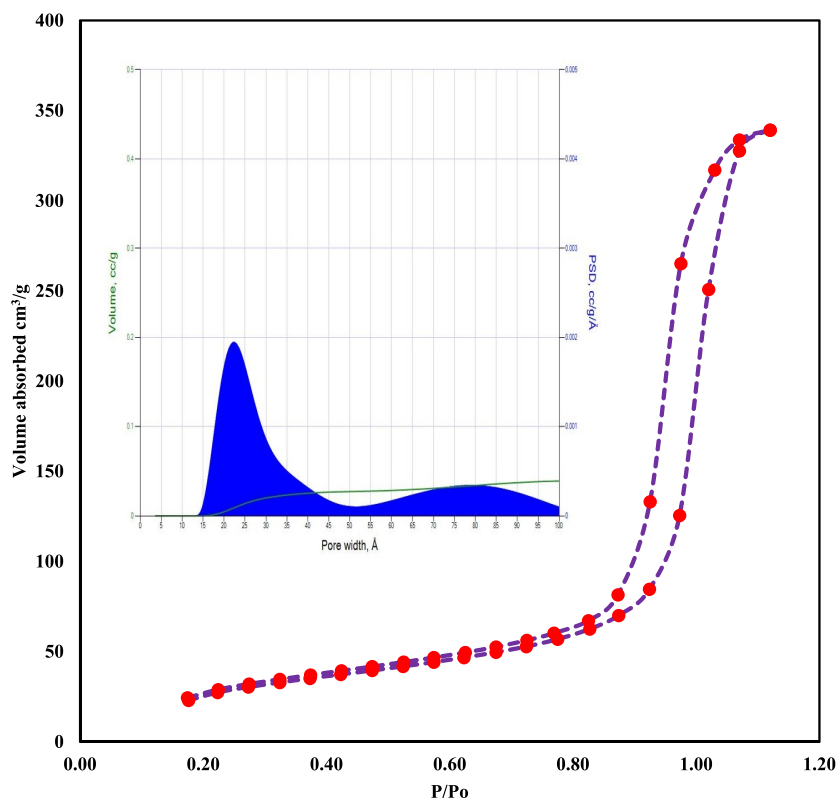


Figure 6. 2D-NLDFT-based pore size distributions.

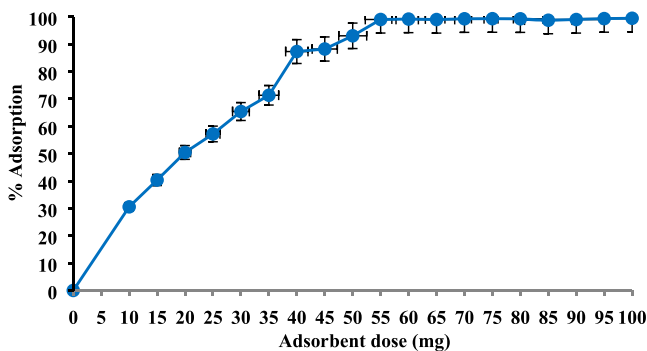


Figure 7. Effect of DIS resin dosages (10 mL of dye, 2×10^{-5} mol/L, 20 min shaking time).

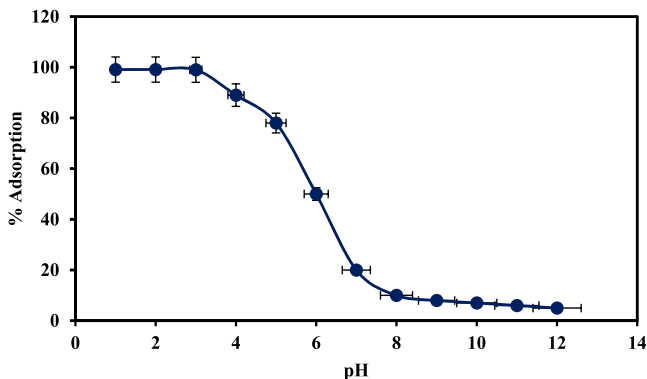


Figure 8. Effect of pH on DB-38 removal from water (10 mL, 2×10^{-5} mol/L, 60 mg of DIS resin)

clearly demonstrates that the adsorption mechanism between DB-38 and the DIS resin is exothermic, the equilibrium was

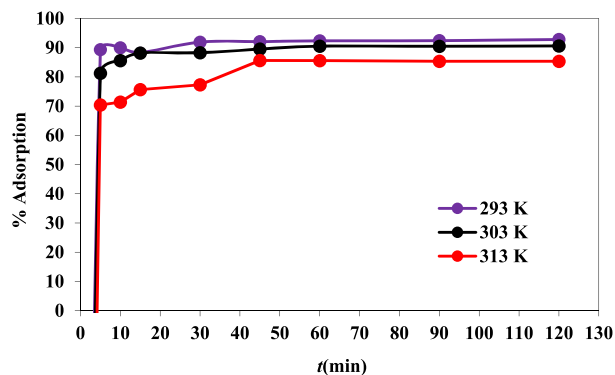


Figure 9. Effect of temperature on % adsorption of the DB-38 dye attached to the DIS resin (10 mL, 2×10^{-5} M, 60 mg of DIS resin).

obtained in 45 min at various temperatures, and further increasing the time up to 45 min has no major effect on the % removal of the DB-38 dye. This may be due to the decrease in the binding forces between the DB-38 dye and DIS resin. Increasing the temperature decreases the dye adsorption, which was reported in different studies. The adsorption of methylene blue has been performed, and it has been observed that the % adsorption decreases with increasing temperature.³⁵ Another study reported that the adsorption of dyes such as methyl violet (MV), methyl green (MG), and methylene blue (MB) decreased with increasing temperature.⁸

5. ADSORPTION ISOTHERM

Isotherm models describe the adsorption phenomenon; therefore, experimental data were subjected to Langmuir, Freundlich, and Dubinin–Radushkevich (D-R) isotherm models and their linear forms are given below in eqs 3–5³⁶

$$\left(\frac{C_e}{C_{\text{ads}}}\right) = \left(\frac{1}{Qb}\right) + \left(\frac{C_e}{Q}\right) \quad (3)$$

$$\log C_{\text{ads}} = \log A + \left(\frac{1}{n}\right) \log C_e \quad (4)$$

$$\ln C_{\text{ads}} = \ln X_m - \beta \varepsilon^2 \quad (5)$$

where C_e (mol/L) is the equilibrium concentration of the DB-38 dye in solution, C_{ads} (mol/g) is the amount of DB-38 dye on the adsorbent surface, Q describes the maximum amount of dye adsorbed, which implies the monolayer coverage of the adsorbent surface, b is a Langmuir constant that shows the binding energy of the dye, A is the Freundlich constant, and $1/n$ shows the adsorption intensity.

Thus, the Langmuir model has been applied by plotting the graph in between C_e/C_{ads} versus C_e , and a straight line has been obtained with its regression coefficient shown in Figure 10. The Langmuir constant values are given in Table 2 and

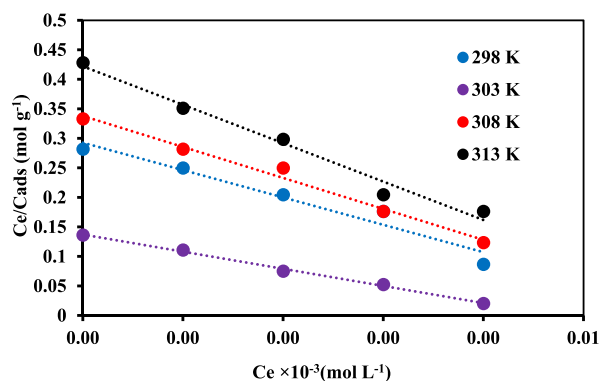


Figure 10. Langmuir graph between C_e (mol/L) and C_e/C_{ads} (2×10^{-9} to 2×10^{-5} mol/L, with 20 min time and 60 mg of DIS resin).

Table 2. Langmuir Isotherm Parameters

temperature	Q (mol/g)	b	R_L	R^2
298	7.28	0.041	0.99–0.21	0.996
303	3.42	0.062	0.99–0.22	0.952
308	2.95	0.065	0.99–0.12	0.987
313	2.36	0.067	0.99–0.13	0.981

obtained from the slope and intercept of the graph. The characteristics of the Langmuir model can be demonstrated by R_L , known as a separation factor and can be calculated using eq 6, where b is a constant and C_i is the initial concentration (Table S4).

$$R_L = \frac{1}{1 + bC_i} \quad (6)$$

The Freundlich isotherm model describes multilayer formation onto an adsorbent surface. In this regard, eq 10 was applied; the graph was plotted between $\log C_{\text{ads}}$ (mol/g) and $\log C_e$ and A and n can be calculated from this graph, which are given in Table S5, Table 3, and Figure 11. The constant parameter values of this model explain that the adsorption follows a multilayer formation rather than the Langmuir model.

The D-R isotherm model is applicable to describe the adsorption nature and calculate energy E (kJ/mol) used in the

Table 3. Freundlich Isotherm Parameters

temperature	A (mg g ⁻¹)	$1/n$	R^2
298	26,696	1.28	0.983
303	7729.0	1.12	0.999
308	3210	1.11	0.999
313	1351	1.10	0.999

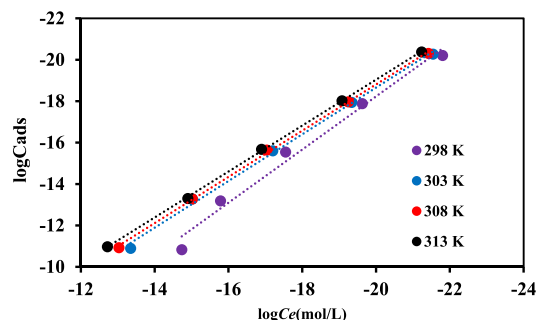


Figure 11. Freundlich model graph between $\log C_e$ (mol/L) and $\log C_{\text{ads}}$ (2×10^{-9} to 2×10^{-5} mol/L, with 20 min time and 60 mg of DIS resin).

adsorption reaction. The very important factor of this model is the Polanyi potential, denoted by (ε), which can be calculated using eq 7.

$$\varepsilon = RT \ln \left(1 + \frac{1}{C_e} \right) \quad (7)$$

where T is the temperature in Kelvin (K), R is the gas constant, which has the unit kJ/mol K, and E describes the mean adsorption energy given in eq 8.

$$E = \frac{1}{\sqrt{-2\beta}} \quad (8)$$

Whenever ε was plotted against $\ln C_{\text{ads}}$ (mol/g), a straight line would be obtained from the diagram with a good correlation coefficient value ($R^2 = 0.999$), which is shown in Table S6 and Figure 12. In Table 4, the values of X_m (mol/g) and E (kJ/mol) demonstrate that the adsorption of the DB-38 dye onto the DIS resin is via resin ion exchange.

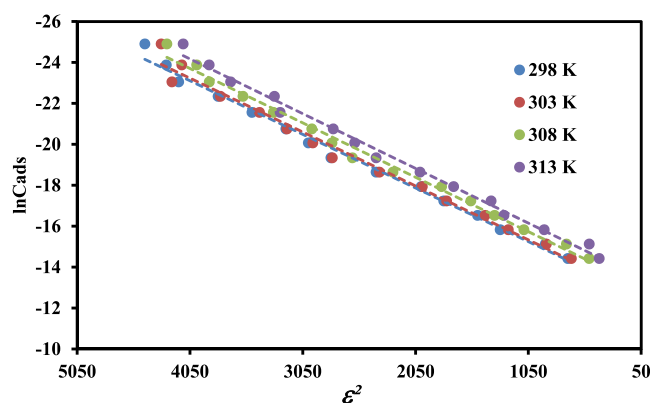


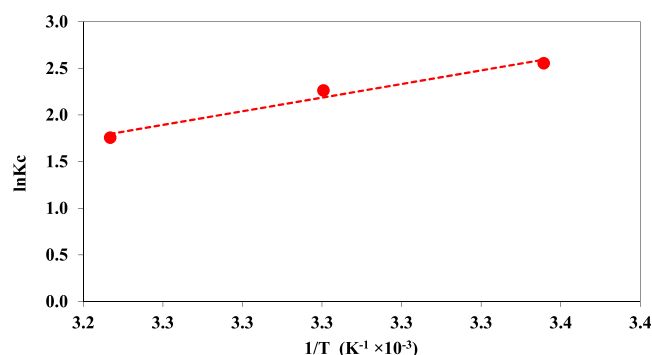
Figure 12. D-R isotherm plot (2×10^{-9} to 2×10^{-5} mol/L, with 20 min time and 60 mg of DIS resin).

Table 4. D-R Isotherm Parameters

temperature	X_m (mmol/g)	E (kJ/mol)	R^2
298	0.183	12.98	0.999
303	0.176	11.91	0.999
308	0.161	11.41	0.999
313	0.153	10.33	0.999

6. THERMODYNAMICS STUDY

A thermodynamics study was performed for the adsorption of the DB-38 dye from water with a temperature range from 293–303 K and a graph was plotted between $\ln k_c$ and $1/T$: a straight line was obtained with a good correlation coefficient ($R^2 = 0.991$) (Figure 13). From the slope and intercept, the

**Figure 13.** Effect of temperature on the adsorption of the DB-38 dye onto the DIS resin.

values of the enthalpy (ΔH) and entropy (ΔS) can be calculated using eq 9 while the Gibbs free energy (ΔG) was calculated using eq 10; and constant parameter values are listed in Table 5.

Table 5. Thermodynamic Constant Parameters for the Adsorption of the DB-38 Dye onto the DIS Resin

ΔH (kJ/mol)	ΔS (kJ/mol/K)	ΔG (kJ/mol)		
		293 K	303 K	308 K
-0.0146	-0.0227	-6.33	-5.70	-4.50
		$\ln k_c = 2.6$	$\ln k_c = 2.3$	$\ln k_c = 1.8$

$$\ln k_c = \frac{-\Delta H}{RT} + \frac{\Delta S}{R} \quad (9)$$

$$\Delta G = RT \ln k_c \quad (10)$$

The numerical values of the thermodynamic parameters are listed in Table 5 in which the negative value of ΔG shows the spontaneity of the DB-38 dye adsorption process onto the DIS resin, while the negative value of ΔH explains that the adsorption reaction is exothermic in nature and the value of $\ln k_c$ decreasing with the rise in temperature shows that the reaction is independent and spontaneous. Moreover, the low ΔS value describes the randomness being increased during the adsorption reaction at the DIS resin surface.

7. REAL WASTEWATER SAMPLE ANALYSIS

The effectiveness of the DIS resin was determined by applying real dye wastewater samples obtained from industrial effluents

in the Hyderabad district, Sindh, Pakistan. The DIS resin (60 mg) was added into 10 mL of dye-contaminated wastewater sample. The results shows that the DIS resin has a good % recovery of 98.9%, and also the values of pH, TDS, conductivity, and salinity of real wastewater samples were normalized after treatments and are given in Table 6.

Table 6. Real Wastewater Sample Values before and after Treatment with DIS Resin

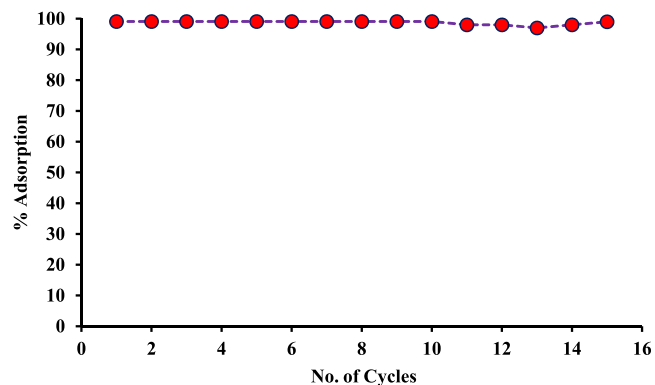
parameter	wastewater before treatment with DIS resin	wastewater after treatment with DIS resin	% recovery
conc (mol/L)	1.2×10^{-4}	2.0×10^{-5}	83.34
	3.2×10^{-4}	2.3×10^{-5}	92.81
	4.5×10^{-4}	2.1×10^{-5}	95.33
pH	9.3	7.8	
	9.8	7.5	
	9.7	7.3	
TDS (mg/L)	360	220	
	450	250	
	430	190	
conductivity ($\mu\text{S/cm}$)	1880.92	430	
	1560.87	320	
	2090.72	490	
salinity	1.9	0.08	
	2.1	0.06	
	1.7	0.07	

8. REUSABILITY OF THE DIS RESIN

The DIS resin can be used many times by washing with methanol and water at a 1:5 ratio, which is the most important feature of this material. Figure 14 clearly shows that there is no change observed in the efficiency of the DIS resin after many cycles confirming its reusability.

9. THEORETICAL EXPLANATION FOR ADSORPTION

In the theoretical part of this study, the optimization of studied dye molecules was performed at the B3LYP/DZP calculation level of the ADF program.³⁷ The power of the interaction

**Figure 14.** Reusability DIS resin after many cycles.

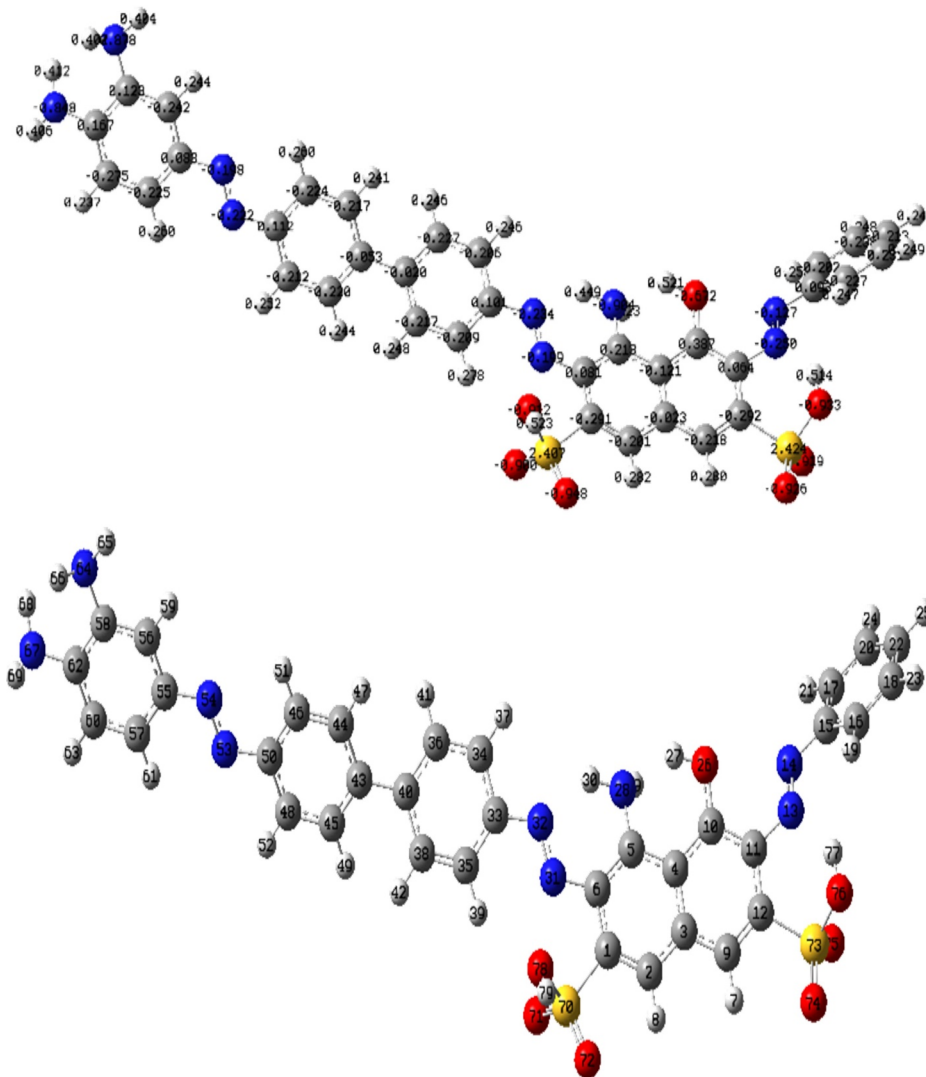


Figure 15. Partial charges on atoms of the dye molecule.

between adsorbent and dye molecules can be determined in the light of chemical reactivity analysis. In conceptual density functional theory,³⁸ chemical reactivity descriptors such as chemical hardness (η), chemical potential (μ), electronegativity (χ), and softness (σ) are defined within the framework of eqs 11–13 based on the ionization energy (I), electron affinity (A), and frontier orbital (HOMO and LUMO) energies of molecules.

$$\chi = -\mu = \left(\frac{I + A}{2} \right) = \frac{-E_{\text{HOMO}} - E_{\text{LUMO}}}{2} \quad (11)$$

$$\eta = \frac{I - A}{2} = \frac{E_{\text{LUMO}} - E_{\text{HOMO}}}{2} \quad (12)$$

$$\sigma = 1/\eta \quad (13)$$

Calculated HOMO and LUMO orbital energies for the studied dye molecule at the aforementioned calculation level are -6.05 and -4.22 eV, respectively. In light of this information, one can say that the chemical hardness value of the dye molecule is 0.915 eV. In many papers written by Kaya and coworkers,^{39,40} chemical hardness is defined as the resistance toward electron cloud polarization or deformation

of chemical species. According to the maximum hardness principle,⁴¹ chemical hardness can be considered as a measure of the stability of chemical species and hard molecules are less reactive than soft molecules. It is apparent from the chemical hardness data obtained for the studied dye molecule that this molecule is very soft and gives the electrons to the adsorbent easily. Hard and soft acid–base principle states that “Hard molecules prefer to coordinate to hard bases and soft molecules prefer to coordinate to soft bases.” In a recent paper, Kokalj⁴² showed that in the explanation of the power of the interactions in the adsorption process, the HSAB principle is very useful. In the same paper, he noted that the HSAB principle estimates the charge transfer between the adsorbate and metal surfaces. In Figure 15, partial charges on atoms of the studied dye molecule are given in detail. In this way, we detected the most suitable regions for the formation of hydrogen bonds. Hydrogen bonds occur as a result of the electrostatic interaction between one electronegative atom and the hydrogen bonded to another electronegative atom. It is important to note that this interaction has a key role in many adsorption processes. The strength of the adsorption between adsorbent and dye molecules can be explained by considering the hydrogen bonds formed.

10. COMPARATIVE STUDY

The synthetic adsorbent plays a very crucial role in the treatment of these toxicants. Therefore, a very huge number of synthetic materials are available and their adsorption efficiencies are comparable with those of the present adsorbent, which are shown in Table 7.

Table 7. Maximum % Adsorption of Different Adsorbents

adsorbent	dyes	% adsorption	refs
<i>p</i> -tert-butylcalix[6]arene-based silica resin	DB-38	91%	28
graphene oxide (GO) salphonated calix[4]arene (SC)	MB, CV, MO, and EY	80–90%	43
CELF aminated lignin product	DB-1	90%	44
Fe ₃ O ₄ /C–COP	auramine O and rhodamine B	95–96%	45
MWCNT-OH–Pd-NPs	malachite Green	96%	46
calix[6]arene-appended XAD-4 resin	RB-5 and DB-38	88%	6
DIS resin	DB-38	99.1%	present study

11. CONCLUSIONS

In this study, the synthesis of the DIS resin and its usage for the adsorption of the DB-38 dye from water are reported. It could be concluded that the adsorption of DB-38 on the DIS resin is pH-dependent. The most effective adsorption of DB-38 has been observed at acidic pH, and further a higher pH is not favorable. The adsorption equilibrium data follow the Freundlich model very well with a good correlation coefficient value, i.e., $R^2 = 0.999$. The adsorption of the DB-38 dye decreased with increasing temperature. The values of ΔH and ΔS are -0.0146 and -0.0227 , respectively, which demonstrate that the adsorption is exothermic and decreases the randomness, while the values of ΔG are -6.12 , -4.19 , and -3.23 , which show that the adsorption is spontaneous. The DIS resin was applied on real wastewater samples too, and it has been found that the DIS resin has very good % recovery. The reusability of the DIS resin shows that there is no significant change in % adsorption or removal efficiency after using many times. The adsorption mechanism was described with the help of DFT calculations, which revealed the chemical nature of the dye and the adsorbent binding energies very well.

■ ASSOCIATED CONTENT

Supporting Information

The Supporting Information is available free of charge at <https://pubs.acs.org/doi/10.1021/acs.jced.0c00292>.

Removal of the DB-38 dye performed at the optimized dosage, pH effect, and temperature optimization and adsorption phenomenon at various concentrations and different temperatures (PDF)

■ AUTHOR INFORMATION

Corresponding Author

Ranjhan Junejo – National Centre of Excellence in Analytical Chemistry, University of Sindh, Jamshoro 76080, Pakistan;
 orcid.org/0000-0002-0090-1146; Email: ranjhanjunejo@yahoo.com

Authors

Shahabuddin Memon – National Centre of Excellence in Analytical Chemistry, University of Sindh, Jamshoro 76080, Pakistan

Savas Kaya – Health Services Vocational School, Department of Pharmacy, Sivas Cumhuriyet University, 58140 Sivas, Turkey

Complete contact information is available at:

<https://pubs.acs.org/10.1021/acs.jced.0c00292>

Notes

The authors declare no competing financial interest.

■ ACKNOWLEDGMENTS

We are thankful to the National Centre of Excellence in Analytical Chemistry, University of Sindh Jamshoro for their support and help.

■ REFERENCES

- (1) Parchebaf Jadid, A.; Nojameh, G. Modified nano- γ -alumina with 2, 4-dinitrophenyl hydrazine as an efficient adsorbent for the removal of everzol red 3BS dye from aqueous solutions. *Eurasian Chem. Commun.* **2019**, *2*, 395–490.
- (2) Liu, X.; Tian, J.; Li, Y.; Sun, N.; Mi, S.; Xie, Y.; Chen, Z. Enhanced dyes adsorption from wastewater via Fe₃O₄ nanoparticles functionalized activated carbon. *J. Hazard. Mater.* **2019**, *373*, 397–407.
- (3) Jiang, C.; Wang, X.; Qin, D.; Da, W.; Hou, B.; Hao, C.; Wu, J. Construction of magnetic lignin-based adsorbent and its adsorption properties for dyes. *J. Hazard. Mater.* **2019**, *369*, 50–61.
- (4) Kambh, M. A.; Solangi, I. B.; Sherazi, S. T. H.; Memon, S. Synthesis and application of calix [4] arene based resin for the removal of azo dyes. *J. Hazard. Mater.* **2009**, *172*, 234–239.
- (5) Gungor, O.; Yilmaz, A.; Memon, S.; Yilmaz, M. Evaluation of the performance of calix [8] arene derivatives as liquid phase extraction material for the removal of azo dyes. *J. Hazard. Mater.* **2008**, *158*, 202–207.
- (6) Memon, S.; Bhatti, A. A.; Bhatti, A. A.; Solangi, I. B. Synthesis and adsorption efficiency of calix [6] arene appended XAD-4 resin. *Desalin. Water Treat.* **2016**, *57*, 1844–1856.
- (7) Erdemir, S.; Bahadir, M.; Yilmaz, M. Extraction of carcinogenic aromatic amines from aqueous solution using calix [n] arene derivatives as carrier. *J. Hazard Mater.* **2009**, *168*, 1170–1176.
- (8) Memon, F. N.; Memon, S. Sorption and desorption of basic dyes from industrial wastewater using calix [4] arene based impregnated material. *Sep. Sci. Technol.* **2015**, *50*, 1135–1146.
- (9) Camel, V. Solid phase extraction of trace elements. *Spectrochim. Acta, Part B* **2003**, *58*, 1177–1233.
- (10) Starvin, A. M. *Offline and online solid phase extraction/preconcentration of inorganics*. Ph. D Thesis, Cochin University of Science and Technology, (Council of Scientific and Industrial Research Regional Research Laboratory Industrial Estate P.O., Thiruvananthapuram - 695019, India, 2005.
- (11) Kambh, M. A.; Solangi, I. B.; Sherazi, S. T. H.; Memon, S. A highly efficient calix [4] arene based resin for the removal of azo dyes. *Desalination* **2011**, *268*, 83–89.
- (12) Memon, S.; Memon, F. N.; Durmaz, F.; Memon, N. A.; Memon, A. A.; Kara, H. Simultaneous determination of some basic dyes using *p*-tetranitrocalix [4] arene-appended silica-based HPLC column. *Anal. Methods* **2014**, *6*, 7318–7323.
- (13) Ghasemi, A. S.; Ashrafi, F.; Tavasoli, T. M.; Hoosini, M.; Norouzi, M.; Karimnia, M.; Sadeghi, A. Studying physicochemical characteristics of Flutamide adsorption on the Zn doped SWCNT (5,5), using DFT and MO calculations. *Eurasian Chem. Commun.* **2020**, *2*, 138–149.
- (14) Afshar, M.; Ranjineh khojasteh, R.; Ahmadi, R. Adsorption of lomustin anticancer drug on the surface of carbon nanotube: A theoretical study. *Eurasian Chem. Commun.* **2020**, *2*, 595–603.

- (15) Parchebaf, A.; Nojameh, G. Modified nano- γ -alumina with 2, 4-dinitrophenyl hydrazine as an efficient adsorbent for the removal of everzol red 3BS dye from aqueous solutions. *Eurasian Chem. Commun.* **2020**, *2*, 475–490.
- (16) Shahzad, H.; Ahmadi, R.; Najafpour, J.; Adhami, F. Adsorption of Cytarabine on the Surface of Fullerene C20: A Comprehensive DFT Study. *Eurasian Chem. Commun.* **2020**, *2*, 162–169.
- (17) Fereydoun Asl, E.; Mohseni-Shahri, F. S.; Moeinpour, F. NiFe₂O₄ coated sand as a nano-adsorbent for removal of Pb (II) from aqueous solutions. *Eurasian Chem. Commun.* **2019**, *1*, 480–493.
- (18) Olasehinde, E. F.; Abegunde, S. M. Adsorption of Methylene Blue onto Acid Modified *Raphia Taedigera* Seed Activated Carbon. *Adv. J. Chem. Sect. A* **2020**.
- (19) Junejo, R.; Memon, S.; Palabiyik, I. M. Efficient adsorption of heavy metal ions onto diethylamine functionalized calix [4] arene based silica resin. *Eurasian Chem. Commun.* **2020**, *2*, 785–797.
- (20) Schalley, C. A. Molecular recognition and supramolecular chemistry in the gas phase. *Mass Spectrom. Rev.* **2001**, *20*, 253–309.
- (21) Morohashi, N.; Narumi, F.; Iki, N.; Hattori, T.; Miyano, S. Thiacalixarenes. *Chem. Rev.* **2006**, *106*, 5291–5316.
- (22) Hutchinson, S.; Kearney, G. A.; Horne, E.; Lynch, B.; Glennon, J. D.; McKervey, M. A.; Harris, S. J. Solid phase extraction of metal ions using immobilised chelating calixarene tetrahydroxamates. *Anal. Chim. Acta* **1994**, *291*, 269–275.
- (23) Junejo, R.; Memon, S.; Memon, F. N.; Memon, A. A.; Durmaz, F.; Bhatti, A. A.; Bhatti, A. A. Thermodynamic and Kinetic Studies for Adsorption of Reactive Blue (RB-19) Dye Using Calix [4] arene-Based Adsorbent. *J. Chem. Eng.* **2019**, *64*, 3407–3415.
- (24) Gutsche, C. D.; Dhawan, B.; No, K. H.; Muthukrishnan, R. Calixarenes. 4. The synthesis, characterization, and properties of the calixarenes from p-tert-butylphenol. *J. Am. Chem. Soc.* **1981**, *103*, 3782–3792.
- (25) Gutsche, C. D.; Lin, L.-G. Calixarenes 12: the synthesis of functionalized calixarenes. *Tetrahedron* **1986**, *42*, 1633–1640.
- (26) Gutsche, C. D.; Nam, K. C. Calixarenes. 22. Synthesis, properties, and metal complexation of aminocalixarenes. *J. Am. Chem. Soc.* **1988**, *110*, 6153–6162.
- (27) Kamboh, M. A.; Solangi, I. B.; Sherazi, S. T. H.; Memon, S. Synthesis and application of p-tert-butylcalix [8] arene immobilized material for the removal of azo dyes. *J. Hazard Mater.* **2011**, *186*, 651–658.
- (28) Kamboh, M. A.; Bhatti, A. A.; Solangi, I. B.; Sherazi, S. T. H.; Memon, S. Adsorption of direct black-38 azo dye on p-tert-butylcalix [6] arene immobilized material. *Arab. J. Chem.* **2014**, *7*, 125–131.
- (29) Goldstein, J. I.; Newbury, D. E.; Michael, J. R.; Ritchie, N. W.; Scott, J. H. J.; Joy, D. C. *Scanning electron microscopy and X-ray microanalysis*. Springer, 2017.
- (30) Bhatti, A. A.; Kamboh, M. A.; Solangi, I. B.; Memon, S. Synthesis of calix [6] arene based XAD-4 material for the removal of reactive blue 19 from aqueous environments. *J. Appl. Polym. Sci.* **2013**, *130*, 776–785.
- (31) Kamboh, M. A.; Wan Ibrahim, W. A.; Rashidi Nodeh, H.; Zardari, L. A.; Sherazi, S. T. H.; Sanagi, M. M. p-Sulphonatocalix-[8]arene functionalized silica resin for the enhanced removal of methylene blue from wastewater: equilibrium and kinetic study. *Sep. Sci. Technol.* **2019**, *54*, 2240–2251.
- (32) Bhatti, A. A.; Oguz, M.; Yilmaz, M. Magnetizing calixarene: Azo dye removal from aqueous media by Fe₃O₄ nanoparticles fabricated with carboxylic-substituted calix [4] arene. *J. Chem. Eng. Data* **2017**, *62*, 2819–2825.
- (33) Memon, S.; Bhatti, A. A.; Bhatti, A. A. Calix [4] arene resin, an efficient adsorbent for azo dyes. *Polycycl Aromat. Compd.* **2019**, *39*, 238–247.
- (34) Güngör, Ö. Efficient removal of carcinogenic azo dyes by novel pyrazine-2-carboxylate substituted calix [4, 8] arene derivatives. *Supramol. Chem.* **2019**, *31*, 776–783.
- (35) de Farias Silva, C. E.; da Gama, B. M. V.; da Silva Gonçalves, A. H.; Medeiros, J. A.; de Souza Abud, A. K. Basic-dye adsorption in albedo residue: Effect of pH, contact time, temperature, dye concentration, biomass dosage, rotation and ionic strength. *J. King Saud Univ. Eng. Sci.* **2019**, 351.
- (36) Mate, C. J.; Mishra, S. Synthesis of borax cross-linked Jhingan gum hydrogel for remediation of Remazol Brilliant Blue R (RBBR) dye from water: Adsorption isotherm, kinetic, thermodynamic and biodegradation studies. *Int. J. Biol. Macromol.* **2020**, *151*, 677–690.
- (37) Te Velde, G. t.; Bickelhaupt, F. M.; Baerends, E. J.; Fonseca Guerra, C.; van Gisbergen, S. J.; Snijders, J. G.; Ziegler, T. Chemistry with ADF. *J. Comput. Chem.* **2001**, *22*, 931–967.
- (38) Islam, N.; Kaya, S. *Conceptual Density Functional Theory and Its Application in the Chemical Domain*; CRC Press: Taylor and Francis group, ISBN 9781771886659, Toronto, 2018.
- (39) Kaya, S.; Kaya, C. A new method for calculation of molecular hardness: a theoretical study. *Comput. Theor. Chem.* **2015**, *1060*, 66–70.
- (40) Kaya, S.; Kaya, C. A simple method for the calculation of lattice energies of inorganic ionic crystals based on the chemical hardness. *Inorg. Chem.* **2015**, *54*, 8207–8213.
- (41) Kaya, S.; Kaya, C.; Islam, N. Maximum hardness and minimum polarizability principles through lattice energies of ionic compounds. *Phys. B* **2016**, *485*, 60–66.
- (42) Kokalj, A. On the HSAB based estimate of charge transfer between adsorbates and metal surfaces. *Chem. Phys.* **2012**, *393*, 1–12.
- (43) Narula, A.; Rao, C. P. Hydrogel of the Supramolecular Complex of Graphene Oxide and Sulfonatocalix [4] arene as Reusable Material for the Degradation of Organic Dyes: Demonstration of Adsorption and Degradation by Spectroscopy and Microscopy. *ACS Omega* **2019**, *4*, 5731–5740.
- (44) Meng, X.; Scheidemann, B.; Li, M.; Wang, Y.-y.; Zhao, X.; Toro-González, M.; Singh, P.; Pu, Y.; Wyman, C. E.; Ozcan, S.; Cai, C. M. Synthesis, Characterization, and Utilization of a Lignin-Based Adsorbent for Effective Removal of Azo Dye from Aqueous Solution. *ACS Omega* **2020**, *5*, 2865–2877.
- (45) Shakeri, S.; Rafiee, Z.; Dashtian, K. Fe₃O₄-Based Melamine-Rich Covalent Organic Polymer for Simultaneous Removal of Auramine O and Rhodamine B. *J. Chem. Eng.* **2020**, *65*, 696–705.
- (46) Borousan, F.; Yousefi, F.; Ghaedi, M. Removal of Malachite Green Dye Using IRMOF-3-MWCNT-OH-Pd-NPs as a Novel Adsorbent: Kinetic, Isotherm, and Thermodynamic Studies. *J. Chem. Eng.* **2019**, *64*, 4801–4814.